Int. J. Environ. Res., 7(4):859-868,Autumn 2013
ISSN: 1735-6865

Seasonal Forecast of Local Lake-Effect Snowfall: The Case of Buffalo, U.S.A.

Hartmann, H.*, Livingston, J. and Stapleton, M.G.

Department of Geography, Geology, and the Environment, Slippery Rock University, Slippery Rock, PA 16057, USA

Received 3 July 2012; Revised 20 May 2013; Accepted 27 May 2013

ABSTRACT: The climate and weather patterns of Buffalo (New York, U.S.A.) are strongly influenced by the city's proximity to Lake Erie. Total monthly snowfall in Buffalo is forecasted using neural network techniques (Multi-Layer Perceptron = MLP) and a multiple linear regression (LR) model. The period of analysis comprises 28 years from January 1982 to December 2009. Input data include: zonal wind speed (u-wind), meridional wind speed (v-wind), air temperature, the geopotential height (GPH) over Lake Erie and the surrounding regions at the 1000 mb -, 925 mb -, 850 mb -, and 700 mb - levels as well as the surface pressure and air temperature, mean water temperature, lake surface water temperatures (LSWT) and the amount of ice coverage of Lake Erie; the 500 mb GPH over James Bay, Canada; and the surface pressure over the North-Central Great Plains. Different lead times of the input variables are tested for their suitability. The most accurate result is obtained by using the MLP with an optimum lead time approach (lead times vary for the different input variables between one and six months). The results of the MLP with six months lead time are in good agreement with observed precipitation records over the study period.

Key words: Seasonal forecast, Snow, Lakes, Neural network analysis, Multiple regression

INTRODUCTION

Lake-effect snowfall is a widely known phenomenon found on the leeward shores of large water bodies. In the Great Lakes region of North America, lake-effect snowfall has been the subject to research for several decades. The occurrence of lake-effect snow has also been examined in other regions of North America such as in the lee regions of the Great Salt Lake (Carpenter, 1993), Lake Tahoe (Cairns *et al.*, 2001), Lake Champlain (Payer *et al.*, 2007; Laird *et al.*, 2009), and the Finger Lakes (Laird *et al*., 2010). Outside of North America less research has focused on this phenomenon. Nevertheless, lake effect-snow has been reported from the lee regions of large water bodies such as Lake Baikal (Obolkin and Potemkin, 2006) and the Aral Sea (Small *et al*., 2001). Lake-effect snow on the eastern side of Nam Co, a much smaller water body on the Tibetan Plateau, has been described by Kropacek *et al.* (2010) and Li *et al.* (2009).

This study focuses on the Great Lakes Region of North America. Here, cold arctic air masses cross the lakes in fall and winter, contributing to the phenomenon (Hjelmfelt, 1990). The relatively warm lakes destabilize the colder lower atmosphere through vertical fluxes of heat and moisture from water to air (Burnett *et al.*, 2003). A 13 °C temperature difference between the lake surface water temperature (LSWT) and the 850 mb layer, which corresponds approximately to a dry adiabatic lapse rate, is considered the minimum difference necessary to initiate lake-effect precipitation (Holroyd, 1971). If the air mass reaching the leeward shore is unstable, upward motion will be enhanced, resulting in the formation of clouds and precipitation. If the temperature in the boundary layer exceeds 0 °C through a sufficient depth, precipitation will most likely fall as rain; if the temperature is cooler, precipitation will most likely fall as snow (Miner and Fritsch, 1997). In the Great Lakes, the leeward shore is east or southeast of each lake, where the prevailing winds are onshore. In general, lake-effect precipitation (including snow and rain) plays an important role in the weather and hydrology of much of the Great Lakes region (Lofgren, 2006). Shallow lakes, such as Lake Erie, tend to freeze over early in mid-winter. This results in a reduction in the amount of heat and moisture available for interaction with the overriding air mass and a cessation of lake-effect snow activity (Niziol, 1987).

An increase in the lake-effect snow along the leeward shores of the Great Lakes was observed throughout most of the twentieth century. The increase was attributed to warmer Great Lakes surface waters and decreased ice cover, both consistent with the

*Corresponding author E-mail:heike.hartmann@sru.edu

upward trend in Northern Hemisphere temperatures (Burnett *et al.*, 2003). Heavy lake-effect snowstorms can damage buildings and vegetation, cause power outages and injuries and disrupt air and ground transportation (Kristovich and Spinar, 2005). The increase in lake-effect snow during the twentieth century along with its damage potential makes it a critical research topic. In the last 20 years, much progress has been made in simulating lake-effect circulations in the Great Lakes region with mesoscale models (Hjemfelt, 1990; Laird *et al.*, 2003a; 2003b). The processes that generate lake-effect snow (Wiggin, 1950; Niziol, 1987; Niziol *et al.*, 1995) have been intensively studied and the forecasts have been significantly improved. Wiggin (1950) listed as basic conditions for lake-effect snow at the eastern end of Lake Erie (1) the presence of a stationary or very slow moving low at 500 mb in vicinity of James Bay, Canada, (2) a strong flow of arctic air over the Great Lakes associated with a surface low that has moved into eastern Canada, (3) a southward extension of a surface low across the Great Lakes, assuring southwest winds over the long axis of Lake Erie. Niziol (1987) provided the following additional conditions: (4) a temperature difference of 13 °C or more between the surface water of the lake and 850 mb, (5) the wind direction from the boundary layer (first 50 mb) through the 850 mb level between 230° and 340° at Lake Erie and between 230° and 80° at Lake Ontario, (6) a directional wind shear of less than 60° between the boundary layer and 700 mb, (7) the existence and height of the low-level inversion with most heavy snowfall occurring when inversion heights top 3 km, (8) a surface high centred over the North-Central Great Plains, (9) cyclonic vorticity advection at 850, 700, and 500 mb, (10) the amount of ice cover on the lake, and (11) the topography. The last factor listed by Niziol (1987) is explained in more detail by Hill (1971). Hill (1971) described that in general orographic effects add 5 to 8 inches (13 to 20 cm) of mean annual snowfall per 100 feet (30 m) increase in elevation and an additional lake-effect could result in up to twice as much accumulation.

While all of the above studies focus on dynamic processes and short-term forecasting of weather patterns covering a comparatively large area, the present study is only the second attempt to forecast total monthly snowfall for a single location at the leeward shore of Lake Erie (a time series recorded at the Buffalo Niagara International Airport weather station is taken as an example) one to several months in advance. Two different stochastic methods are tested for their suitability, a multiple linear regression and an artificial neural network. The current approach produces results consistent with Hartmann (2012) with considerable simplification in the model architecture and the input variables. This approach increases the potential warning time for a lake-effect snow event, which may allow improvements in emergency management procedures such as an early allocation of NYS OEM (New York State Office of Emergency Management) and military resources.

MATERIALS & METHODS

All data series used in this study consist of monthly averages or totals and cover the period from January 1982 to December 2009. The authors limited the period of analysis to this period according to the length of available LSWTs and ice concentrations. The time series of total monthly snowfall from Buffalo Niagara International Airport (New York) was used as model output. The time series was downloaded from the data set DS-3220 provided by the National Climatic Data Center, Asheville (North Carolina), USA. Carrying out seasonal forecasts for a single location and concentrating on a monthly time scale enables a certain amount of generalization of the model input; e.g. the topography remains unchanged so this parameter does not need to be implemented to the models. After careful consideration of the variables that were classified as important for short-term forecasts in the above named studies, the following variables were chosen as model input: the u-wind, the v-wind, the air temperature, the geopotential height (GPH) over Lake Erie and the surrounding regions at the 1000 mb -, 925 mb -, 850 mb -, and 700 mb - levels as well as the surface pressure and air temperature; the 500 mb GPH over James Bay, Canada; the surface pressure over the North-Central Great Plains; the mean water temperature, the LSWTs and the amount of ice coverage of Lake Erie.

U-wind, v-wind, air temperature, GPH, and surface pressure of the different levels were taken from NCEP/NCAR Reanalysis 1 (Kalnay *et al.*, 1996; Kistler *et al.*, 2001), provided by the NOAA/OAR/ESRL PSD, Boulder, Colorado, USA at http://www.cdc.noaa.gov. The Lake Erie water temperature, taken at the Buffalo Water Treatment Plant, was provided by the National Weather Service, Buffalo Weather Forecast Office at http://www.wbuf.noaa.gov/laketemps. The reading is taken at a depth of 9.14 m.

LSWTs and ice concentrations (percentage of area covered by ice) were taken from the data set NOAA Optimum Interpolation (OI) Sea Surface Temperature (SST) V2 (Reynolds *et al.*, 2002), which is provided by the NOAA/OAR/ESRL PSD, Boulder, Colorado, USA at http://www.esrl.noaa.gov/psd/. Fig.1, shows the location of the weather station, the Buffalo Water Treatment Plant, and the used grid cells of the NCEP/NCAR Reanalysis 1 and NOAA OI SST V2 data sets.

The low resolution of the grid data did not facilitate a detailed analysis of the meso-scale atmospheric circulation. However, this lies beyond the aim of this study and higher resolution data can be employed at a later point in time.

Data preprocessing included rescaling the time series, which were used as input variables, to the interval [0.1, 0.9] to enable the modelling of extreme events occurring outside the range of the training data (Dawson and Wilby, 2001). Following rescaling the data was split into three data sets: a "training" data set, a "cross-validation" data set, and a "testing" data set. In this study "cross-validation" and "testing" are defined as follows.

"Cross-validation" describes the procedure of avoiding over fitting by determining when the network has been trained as well as possible. The cross-validation data set is used by the network during training. At regular intervals during training of the training data set, the network performance is evaluated on the cross-validation set. During this evaluation, the performance of the network on the cross-validation set is saved and compared to past values. If the network is starting to over-train on the training data, the cross-validation performance will begin to degrade and the training procedure will be stopped (Principe *et al.*, 2005). This definition of "cross-validation" has been used in several studies including Coulibaly *et al.* (2000), and Kang *et al.* (2006). Instead of "cross-validation", Dawson and Wilby (2001) used the term "testing"; in ASCE (2000) this procedure was named "cross training".

"Testing" is used to describe the evaluation of the chosen model against independent data, as was done in various other studies, such as Backhaus *et al.* (2003), and Principe *et al.* (2005). Testing in this study is consistent with the term "validation" as used by Maier and Dandy (2000) and Dawson and Wilby (2001).

The question of how best to divide the data into these data sets is often discussed in the literature (e.g. Gardner and Dorling, 1998; Silverman and Dracup, 2000; Sahai *et al.*, 2003). This study used 80% of the data for training, 10% for cross-validation, and 10% for testing, following the recommendation of Backhaus *et al.* (2003). In general, it is not recommended that the data be randomly sampled. There is a chance that the data in one of the sets may be biased towards extreme or uncommon events, which will cause problems when assessing the performance of the network, as a network can only generalize on the range of data inputs for which it was trained (Gardner and Dorling, 1998). The authors used data for the period from 1982 to 2003 for training, for the period from 2004 to 2006 for cross-validation, and for the period from 2007 to 2009 for testing. To determine the optimum lead time between the input variables and the model output, Spearman's rank correlation coefficients ρ between all of the input variables and the output variable were calculated by making use of the training data set (Table 1).

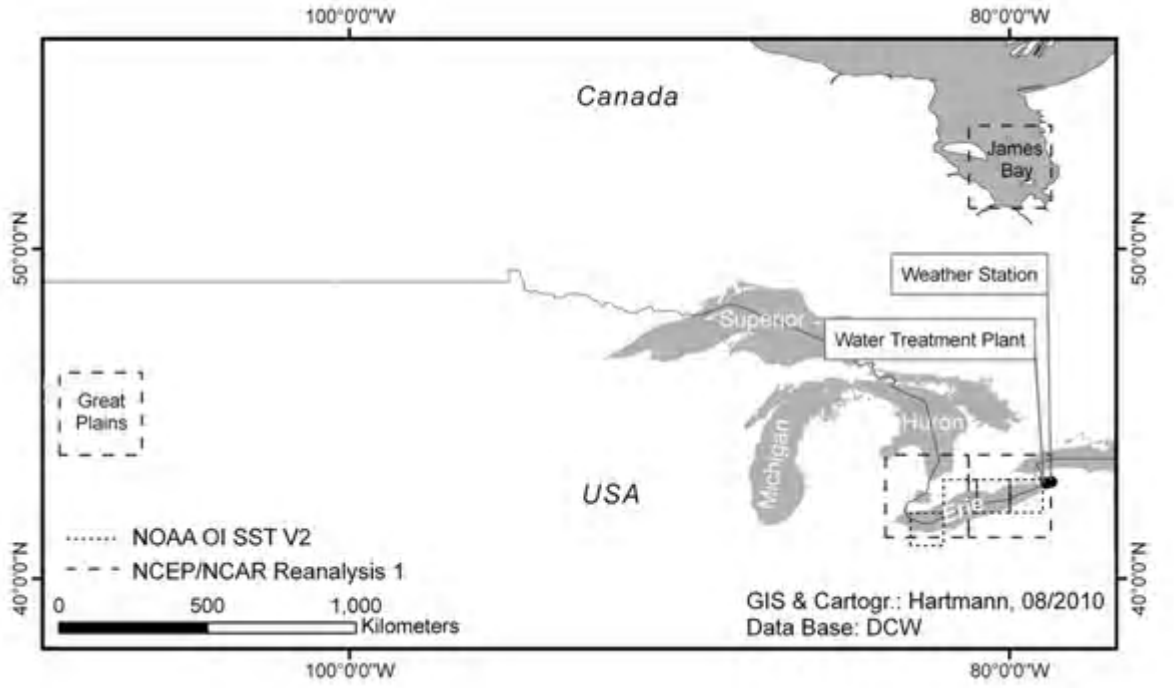

Fig. 1. Location of the Buffalo Niagara International Airport weather station, the Buffalo Water Treatment Plant, and the used grid cells of the NCEP/NCAR Reanalysis 1 and NOAA OI SST V2 data sets

Table 1. Spearman's rank correlation coefficients ñ between total monthly snowfall at Buffalo Niagara International Airport and the various input variables

	LakeT	LakeST	SeaIce	AirT	AirT1000	AirT925	AirT850	AirT700	UWind1000W
Snow lt 0	**-0.80**	**-0.52**	**0.38**	**-0.90**	**-0.90**	**-0.90**	**-0.90**	**-0.90**	**0.53**
Snow lt 1	**-0.53**	-0.10	0.01	**-0.77**	**-0.77**	**-0.77**	**-0.75**	**-0.72**	**0.57***
Snow lt 2	-0.13	**0.36**	**-0.33**	**-0.47**	**-0.48**	**-0.47**	**-0.45**	**-0.40**	**0.49**
Snow lt 3	0.34	**0.71**	**-0.56**	-0.02	-0.03	-0.02	-0.01	0.05	**0.25**
Snow lt 4	**0.70**	**0.87***	**-0.67***	**0.45**	**0.44**	**0.44**	**0.44**	**0.49**	-0.01
Snow lt 5	**0.87***	**0.81**	**-0.64**	**0.77**	**0.76**	**0.77**	**0.76**	**0.79**	**-0.24**
Snow lt 6	**0.82**	**0.54**	**-0.43**	**0.87***	**0.87***	**0.87***	**0.87***	**0.86***	**-0.40**

	UWind1000E	UWind925W	UWind925E	UWind850W	UWind850E	UWind700W
Snow lt 0	**0.47**	**0.50**	**0.50**	**0.53**	**0.56**	**0.60**
Snow lt 1	**0.51***	**0.63***	**0.62***	**0.65***	**0.65***	**0.66***
Snow lt 2	**0.43**	**0.60**	**0.56**	**0.57**	**0.56**	**0.54**
Snow lt 3	**0.22**	**0.32**	**0.29**	**0.26**	**0.24**	**0.19**
Snow lt 4	-0.02	0.03	0.01	-0.04	-0.08	-0.13
Snow lt 5	**-0.22**	**-0.21**	**-0.23**	**-0.29**	**-0.32**	**-0.40**
Snow lt 6	**-0.37**	**-0.42**	**-0.43**	**-0.48**	**-0.50**	**-0.57**

	UWind700E	VWind1000W	VWind1000E	VWind925W	VWind925E	VWind850W
Snow lt 0	**0.62**	**0.24**	**0.23**	**0.18**	0.15	0.00
Snow lt 1	**0.66***	**0.49**	**0.48**	**0.39**	**0.35**	0.15
Snow lt 2	**0.52**	**0.58***	**0.59***	**0.45***	**0.46***	**0.25***
Snow lt 3	**0.18**	**0.40**	**0.43**	**0.28**	**0.32**	**0.20**
Snow lt 4	-0.15	**0.20**	**0.21**	0.08	0.12	0.10
Snow lt 5	**-0.41**	-0.01	0.02	-0.09	-0.03	-0.01
Snow lt 6	**-0.58**	**-0.21**	**-0.18**	**-0.24**	**-0.17**	-0.08

	VWind850E	VWind700W	VWind700E	GPH1000	GPH925	GPH850
Snow lt0	-0.01	0.09	0.12	0.13	**-0.70**	**-0.86**
Snow lt1	0.12	**0.22**	**0.23**	**0.36**	**-0.40**	**-0.62**
Snow lt2	**0.27***	**0.33***	**0.36***	**0.44***	-0.08	**-0.27**
Snow lt3	**0.23**	**0.25**	**0.29**	**0.40**	**0.28**	0.15
Snow lt4	0.14	0.10	0.14	**0.28**	**0.58**	**0.55**
Snow lt5	0.04	-0.05	0.00	0.07	**0.73***	**0.79**
Snow lt6	-0.03	-0.14	-0.12	**-0.19**	**0.63**	**0.80***

	GPH700	GPH500James	SLPPlains	SLP
Snow lt 0	**-0.89**	**-0.88**	**0.77**	-0.03
Snow lt 1	**-0.69**	**-0.76**	**0.80***	**0.23**
Snow lt 2	**-0.36**	**-0.48**	**0.64**	**0.36**
Snow lt 3	0.08	-0.02	**0.31**	**0.40***
Snow lt 4	**0.52**	**0.43**	-0.08	**0.35**
Snow lt 5	**0.79**	**0.73**	**-0.46**	**0.20**
Snow lt 6	**0.84***	**0.85***	**-0.74**	-0.04

* highest correlation for lt 1 to lt 6

$\rho \geq 0.13$: significant at 95% confidence level – shown in italics

$\rho \geq 0.16$: significant at 99% confidence level- shown in bold italics

LakeT = Lake Erie Water Temperature
LakeST = Lake Erie Surface Temperature
SeaIce = Ice Concentration over Lake Erie
AirT = Surface Air Temperature over Lake Erie and the surrounding regions
AirT1000 = Air Temperature at 1000 mb over Lake Erie and the surrounding regions
AirT925 = Air Temperature at 925 mb over Lake Erie and the surrounding regions
AirT850 = Air Temperature at 850 mb over Lake Erie and the surrounding regions
AirT700 = Air Temperature at 700 mb over Lake Erie and the surrounding regions
UWind1000W = U-Wind at 1000 mb over the western part of Lake Erie
UWind1000E = U-Wind at 1000 mb over the eastern part of Lake Erie
UWind925W = U-Wind at 925 mb over the western part of Lake Erie
UWind925E = U-Wind at 925 mb over the eastern part of Lake Erie
UWind850W = U-Wind at 850 mb over the western part of Lake Erie
UWind850E = U-Wind at 850 mb over the eastern part of Lake Erie
UWind700W = U-Wind at 700 mb over the western part of Lake Erie
UWind700E = U-Wind at 700 mb over the eastern part of Lake Erie
VWind1000W = V-Wind at 1000 mb over the western part of Lake Erie
VWind1000E = V-Wind at 1000 mb over the eastern part of Lake Erie
VWind925W = V-Wind at 925 mb over the western part of Lake Erie
VWind925E = V-Wind at 925 mb over the eastern part of Lake Erie
VWind850W = V-Wind at 850 mb over the western part of Lake Erie
VWind850E = V-Wind at 850 mb over the eastern part of Lake Erie
VWind700W = V-Wind at 700 mb over the western part of Lake Erie
VWind700E = V-Wind at 700 mb over the eastern part of Lake Erie
GPH1000 = Geopotential Height at 1000 mb over Lake Erie and the surrounding regions
GPH925 = Geopotential Height at 925 mb over Lake Erie and the surrounding regions
GPH850 = Geopotential Height at 850 mb over Lake Erie and the surrounding regions
GPH700 = Geopotential Height at 700 mb over Lake Erie and the surrounding regions
GPH500James = Geopotential Height at 500 mb over James Bay, Canada
SLPPlains = Sea Level Pressure over the Great Plains
SLP = Sea Level Pressure over Lake Erie and the surrounding regions

Total monthly snowfall one to several months in advance was predicted applying a linear (multiple linear regressions) as well as a non-linear (artificial neural networks) method. The latter is supposed to be more suitable for reliable forecasts, as the relationships between climatic variables are known to be complex and often non-linear (Cannon and McKendry, 2002). An artificial neural network can be understood as a set of non-linear equations used to obtain the output variable(s) from the input variables (Ashrafi *et al*., 2012). Neural networks are parallel computing structures of processing elements (neurons), which are interconnected by a network similar to the human brain (Hsieh and Tang, 1998). A conventional Multi-Layer Perceptron (MLP) neural network design was applied in the analyses. A MLP is a so-called "feed-forward" neural network because all information flows in one direction. The neurons of one layer are connected to the neurons of the following layer without feedback (Teschl and Randeu, 2006). The signals flowing on the connections are scaled by adjustable parameters called weights (Principe *et al.*, 2000). The weights adjustment was performed by a back propagation algorithm: weights are modified to reduce the error occurrence between actual and desired network outputs backward from the output layer to the input layer (Backhaus *et al.*, 2003). As in Hartmann *et al.* (2008a; 2008b) the architecture of the MLP was determined by a "trial and error" approach. The starting point was a small network consisting of one hidden layer with four neurons. The number of neurons was increased by increments of two for the range from 4 neurons to 30 neurons. The root mean square error (RMSE) in the training data was evaluated and showed its lowest value for 10 neurons. After this, a second hidden layer was implemented and the performance was tested; however, no improvement was achieved. The overall lowest RMSE was produced from a one hidden-layer structure with 10 neurons, therefore this architecture was chosen. Hyperbolic tangent activation

functions were used for the hidden and output layers. Lastly, a multiple linear regression (LR) analysis was carried out and the performances of the analyses were compared.

The modelling of snow was carried out for all months of the year. In addition to assessing the accuracy of the predictions for the snow season, this facilitated testing whether the model was able to predict whether or not snow occurred. To avoid the prediction of negative values during summer, a zero threshold was implemented, which automatically corrected negative values of snow to zero. The performance of the different models was assessed by calculating the correlation coefficient r, the root mean squared error RMSE, the mean absolute error MAE, and the Maximum Absolute Error (MAXAE).

RESULTS & DISCUSSION

The Spearman's rank correlation coefficients ρ between total monthly snowfall at Buffalo and the various input variables (Table 1) show the highest correlation for a lead time of one month for all of the u-wind indices, and the sea level pressure from the Great Plains. The highest correlation for a lead time of two months can be seen for all of the v-wind indices, and the 1000 mb GPH. Only one of the 31 input variables shows the highest correlation coefficient for a lead time of three months, and two for lead times of four and of five months. For eight of the 31 input variables – all of the air temperature indices as well as most of the GPH indices – the highest correlation coefficients were found for a lead time of six months. According to these results, snowfall was modelled with four different lead times: one month (lt 1); two months (lt 2); six months (lt 6); and with the lead time showing the highest correlation coefficient for each of the variables (opt lt).

Table 2 shows a performance comparison of the two different models for the testing, training, and cross-validation period including the four selected lead times. For the testing period, the results are displayed in Fig. 2 (a-h). From Fig. 2 it becomes apparent that the LR

Table 2. Performance comparison of the different models for a) the testing, b) the training, and c) the cross-validation period with lead times of one month (lt 1), two months (lt 2), six months (lt 6), and optimum lead time (opt lt)

a)

TESTING		r	RMSE (mm)	MAE (mm)	MAXAE (mm)
lt 1	MLP	0.78	210.33	130.71	703.35
	LR	0.67	264.85	202.06	826.67
lt 2	MLP	0.76	212.27	119.94	785.85
	LR	0.81	202.01	128.21	702.59
lt 6	MLP	0.83	182.28	113.55	466.75
	LR	0.81	197.24	125.4	625.45
opt lt	MLP	0.9	145.16	84.49	428.84
	LR	0.87	173.95	117.8	646.13

b)

TRAINING		r	RMSE (mm)	MAE (mm)	MAXAE (mm)
lt 1	MLP	0.77	217.69	118.84	1350.71
	LR	0.75	227.37	129.53	1356.73
lt 2	MLP	0.76	222.27	121.05	1017.7
	LR	0.73	234.68	131.9	1377.24
lt 6	MLP	0.74	230.26	118.99	1336.17
	LR	0.73	234.79	127.37	1504.34
opt lt	MLP	0.8	205.56	108.83	1314.28
	LR	0.76	223.48	126.77	1420.35

c)

CROSS-VALIDATION		r	RMSE (mm)	MAE (mm)	MAXAE (mm)
lt 1	MLP	0.92	155.4	88.44	632.49
	LR	0.78	202.23	157.25	519.15
lt 2	MLP	0.86	188.36	112.81	739.43
	LR	0.72	226.51	145.74	738.51
lt 6	MLP	0.87	156.03	91.66	415.65
	LR	0.84	173.47	121.18	482.58
opt lt	MLP	0.83	184.36	102.81	542.16
	LR	0.75	212.95	136.34	587.98

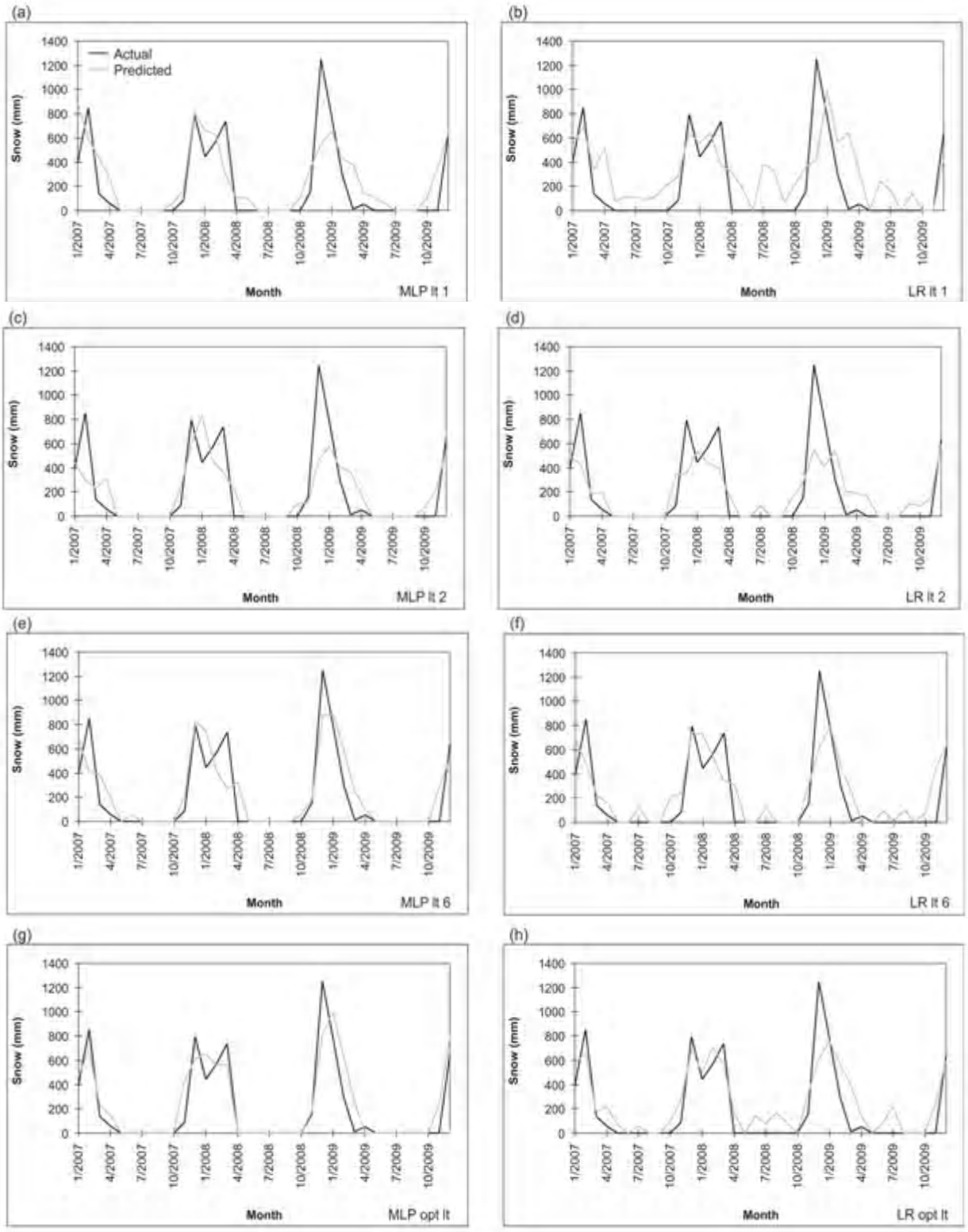

Fig. 2. Actual (in black) and predicted (in grey) total monthly snowfall at Buffalo Niagara International Airport for the test period from January 2007 to December 2009 obtained by two stochastic models with different lead times: (a) MLP with lead time of one month (lt 1), (b) LR with lead time of one month (lt 1), (c) MLP with lead time of two months (lt 2), (d) LR with lead time of two months (lt 2), (e) MLP with lead time of six months (lt 6), (f) LR with lead time of six months (lt 6), (g) MLP with optimum lead time (opt lt), (h) LR with optimum lead time (opt lt)

model is not always able to recognize the snow-free season from the input data. The MLP model works better in this regard. For the lead time of one month, the MLP model (Fig. 2a) is fairly able to simulate the snow-free season, however, it fails to reproduce the maximum in December 2008. The MAXAE is 123.32 mm smaller than the MAXAE for the LR model (Fig. 2b) for the same lead time; however, with the input of December 2009, the LR model produced a high peak one month later in January 2009. With regard to the other error measures and the training and cross-validation results, the authors conclude that both of the models do not simulate the reality successfully. This is also true for the models with a lead time of two months (Fig. 2c, 2d). Both are not able to simulate the maximum in December 2008. The results obtained for a lead time of six months look very promising. This is especially true for the MLP model (Fig. 2e). The snow-free season is recognized and the maxima are fairly well simulated. The MAXAE can be seen again in December 2008, however with 466.75 mm it is comparatively well simulated. With r=0.83 for the test period, r=0.74 for the training and r=0.87 for the cross-validation period, good modelling results have been achieved. The LR model (Fig. 2f) approach with a lead time of six months is far less successful showing a MAXAE of 625.45 mm for December 2008. A result for the MLP that is slightly better (Fig. 2g) can be seen with the optimum lead time approach. The MAXAE drops to 428.84 mm and r rises to r=0.9 for the test period, r=0.8 for the training period, and r=0.83 for the cross-validation period. Even though the r value of 0.87 for the test period simulated by the LR model (Fig. 2h) suggests a fairly good result, the simulation result for December 2008 is not satisfactory (MAXAE=646.13 mm).

The poor results in the training data set with regard to the MAXAEs are largely due to the absolute maximum of the snow time series falling within this data set (2100 mm in December 2001). This value has been underestimated by the models causing large MAXAEs. However, it can be taken from Table 2 that the other error measures (r, RMSE, and MAE) do not differ very much for the different data sets.

It is difficult to compare the results of the current study with the only other study of local monthly lake-effect snowfall (Hartmann, 2012). In Hartmann (2012), additional input variables such as the North Atlantic Oscillation (NAO), Arctic Oscillation (AO), Pacific-North American Pattern (PNA), Southern Oscillation Index (SOI), and Pacific Decadal Oscillation (PDO) were implemented; moreover, different time periods for training, cross-validation, and testing were chosen. By comparing the error measures of the present study with those presented in Hartmann (2012), we notice rather small deviations, even though the above mentioned large-scale circulation patterns were not implemented and the architecture of the MLP was simpler in the present study. It indicates the importance of regional climatic variables over large-scale circulation patterns in this setting.

CONCLUSION

In this study, two different stochastic methods, an artificial neural network (MLP) and a multiple linear regression, were tested for their suitability in forecasting total monthly snowfall for Buffalo one to several months in advance. The most accurate result was obtained using the MLP with an optimum lead time approach. The outcome of the MLP with a lead time of six months was also very successful. The longer warning time enabled by a six month forecast could be viewed as more important than the better accuracy obtained by the MLP with an optimum lead time approach which allowed for only one month advance forecasting. Overall, the introduced method enables an increase of the warning time for a lake-effect snow event, which may allow an improvement in emergency management procedures.

ACKNOLEDGEMENTS

This research was supported by a grant from the College of Health, Environment and Science of Slippery Rock University.

REFERENCES

ASCE, (2000). American Society of Civil Engineers, Artificial Neural Networks in Hydrology. I: Preliminary Concepts. J. Hydrol. Eng., **5 (2),** 115-123.

Ashrafi, K., Shafiepour, M., Ghasemi, L. and Najar Araabi, B. (2012). Prediction of Climate Change Induced Temperature Rise in Regional Scale Using Neural Network. Int. J. Environ. Res., **6 (3),** 677-688.

Backhaus, K., Erichson, B., Plinke, W. and Weiber, R. (2003). Multivariate Analysemethoden. Berlin: Springer.

Burnett, A. W., Kirby, M. E., Mullins, H. T. and Patterson, W. P. (2003). Increasing Great Lake-Effect Snowfall during the Twentieth Century: A Regional Response to Global Warming? J. Clim., **16 (21),** 3535-3542.

Cairns, M. M., Collins, R., Cylke, T., Deutschendorf, M. and Mercer, D. (2001). A lake effect snowfall in Western Nevada - Part I: Synoptic setting and observations. Paper presented at the 18th Conference on Weather Analysis and Forecasting/14th Conference on Numerical Weather Prediction, Fort Lauderdale.

Cannon, A. J. and McKendry, I. G. (2002). A graphical sensitivity analysis for statistical climate models: application to Indian monsoon rainfall prediction by neural networks

and multiple linear regression models. Int. J. Climatol., **22 (13)**, 1687-1708.

Carpenter, D. M. (1993). The Lake Effect of the Great Salt Lake: Overview and Forecast Problems. Weather Forecast., **8 (2)**, 181-193.

Coulibaly, P., Anctil, F. and Bobée, B. (2000). Daily reservoir inflow forecasting using artificial neural networks with stopped training approach. J. Hydrol., **230 (3-4)**, 244-257.

Dawson, C. W. and Wilby, R. L. (2001). Hydrological modelling using artificial neural networks. Prog. Phys. Geog., **25 (1)**, 80-108.

Gardner, M. W. and Dorling, S. R. (1998). Artificial Neural Networks (the Multilayer Perceptron) – A Review of Applications in the Atmospheric Sciences. Atmos. Environ., **32 (14-15)**, 2627-2636.

Hartmann, H. (2012). Neural Network Based Seasonal Predictions of Lake-Effect Snowfall. Atmos.-Ocean, **50 (1)**, 31-41.

Hartmann, H., Becker, S. and King, L. (2008a). Predicting summer rainfall in the Yangtze River basin with neural networks. Int. J. Climatol., **28 (7)**, 925-936.

Hartmann, H., Becker, S., King, L. and Jiang, T. (2008b). Forecasting water levels at the Yangtze River with neural networks. Erdkunde, **62 (3)**, 231-243.

Hill, J. D. (1971). Snow Squalls in the Lee of Lake Erie and Lake Ontario. NOAA Tech. Memo. NWS ER-43.

Hjelmfelt, M. R. (1990). Numerical Study of the Influence of Environmental Conditions on Lake-Effect Snowstorms over Lake Michigan. Mon. Weather Rev., **118 (1)**, 138-150.

Holroyd, E. W. III. (1971). Lake effect cloud bands as seen from weather satellites. J. Atmos. Sci., **28 (7)**, 1165-1170.

Hsieh, W. W. and Tang, B. (1998). Applying Neural Network Models to Prediction and Data Analysis in Meteorology and Oceanography. Bull. Amer. Meteor. Soc., **79 (9),** 1855-1870.

Kalnay, E., Kanamitsu, M., Kistler, R., Collins, W., Deaven, D., Gandin, L., Iredell, M., Saha, S., White, G., Woollen, J., Zhu, Y., Leetmaa, A., Reynolds, R., Chelliah, M., Ebisuzaki, W., Higgins, W., Janowiak, J., Mo, K. C., Ropelewski, C., Wang, J., Jenne, R. and Joseph, D. (1996). The NCEP/ NCAR 40-year reanalysis project. Bull. Amer. Meteor. Soc., **77 (3)**, 437-470.

Kang, M. S., Kang, M. G., Park, S. W., Lee, J. J. and Yoo, K. H. (2006). Application of grey model and artificial neural networks to flood forecasting. J. Am. Water. Resour. Assoc., **42 (2)**, 473-486.

Kistler, R., Kalnay, E., Collins, W., Saha, S., White, G., Woollen, J., Chelliah, M., Ebisuzaki, W., Kanamitsu, M., Kousky, V., van den Dool, H., Jenne, R. and Fiorino, M. (2001). The NCEP-NCAR 50-Year Reanalysis: Monthly Means CD-ROM and Documentation. Bull. Amer. Meteor. Soc., **82 (2)**, 247-267.

Kristovich, D. A. R and Spinar, M. L. (2005). Diurnal Variations in Lake-Effect Precipitation near Western Great Lakes. J. Hydrometeor., **6 (2)**, 210-218.

Kropacek, J., Feng, C., Alle, M., Kang, S. and Hochschild, V. (2010). Temporal and Spatial Aspects of Snow Distribution in the Nam Co Basin on the Tibetan Plateau from MODIS Data. Remote Sens., **2 (12)**, 2700-2712.

Laird, N. F., Desrochers, J. and Payer, M. (2009). Climatology of Lake-Effect Precipitation Events over Lake Champlain. J. Appl. Meteor. Climatol., **48 (2)**, 232-250.

Laird, N. F., Kristovich, D. A. R. and Walsh, J. E. (2003a). Idealized Model Simulations Examining the Mesoscale Structure of Winter Lake-Effect Circulations. Mon. Weather Rev., **131 (1)**, 206-221.

Laird, N. F., Sobash, R. and Hodas, N. (2010). Climatological Conditions of Lake-Effect Precipitation Events Associated with the New York State Finger Lakes. J. Appl. Meteor. Climatol., **49 (5)**, 1052-1062.

Laird, N. F., Walsh, J. E. and Kristovich, D. A. R. (2003b). Model simulations examining the Relationship of Lake-Effect Morphology to Lake Shape, Wind Direction, and Wind Speed. Mon. Weather Rev., **131 (9)**, 2102-2111.

Li, M., Ma, Y., Hu, Z., Ishikawa, H. and Oku, Y. (2009). Snow distribution over the Namco lake area of the Tibetan Plateau. Hydrol. Earth Syst. Sci., **13 (11)**, 2023-2030.

Lofgren, B. M. (2006). Land Surface Roughness Effects on Lake Effect Precipitation. J. Great Lakes Res., **32 (4)**, 839-851.

Maier, H. R. and Dandy, G. C. (2000). Neural networks for the prediction and forecasting of water resources variables: a review of modelling issues and applications. Environ. Model. Softw., **15 (1)**, 101-124.

Miner, T. J. and Fritsch, J. M. (1997). Lake-Effect Rain Events. Mon. Weather Rev., **125 (12)**, 3231-3248.

Niziol, T. A. (1987). Operational forecasting of lake effect snow in western and central New York. Weather Forecast., **2 (4)**, 310-321.

Niziol, T. A., Snyder, W. R. and Waldstreicher, J. S. (1995): Winter Weather Forecasting throughout the Eastern United States. Part IV: Lake Effect Snow. Weather Forecast., **10 (1)**, 61-77.

Obolkin, V. A. and Potemkin, V. L. (2006). The impact of large lakes on climate in the past: a possible scenario for Lake Baikal. Hydrobiologia, **568 (S1)**, 249-252.

Payer, M., Desrochers, J. and Laird, N. F. (2007): A Lake-Effect Snowband over Lake Champlain. Mon. Wea. Rev., **135 (11)**, 3895–3900.

Principe, J. C., Euliano, N. R. and Lefebvre, W. C. (2000). Neural and Adaptive Systems – Fundamentals Through Simulations. New York: Wiley.

Principe, J., Lefebvre, C., Lynn, G., Fancourt, C. and Wooten, D. (2005). NeuroSolutions–Documentation. Gainesville: NeuroDimension, Inc.

Reynolds, R. W., Rayner, N. A., Smith, T. M., Stokes, D. C. and Wang, W. (2002). An improved in situ and satellite SST analysis for climate. J. Clim., **15 (13)**, 1609-1625.

Sahai, A. K., Pattanaik, D. R., Satyan, V. and Grimm, A. M. (2003). Teleconnections in recent time and prediction of Indian summer monsoon rainfall. Meteor. Atmos. Phys., **84 (3-4)**, 217-227.

Silverman, D. and Dracup, J. (2000). Artificial Neural Networks and Long Range Precipitation Prediction in California. J. Appl. Meteor., **39 (1)**, 57-66.

Small, E. E., Giorgi, F., Sloan, L. C. and Hostetler, S. (2001). The Effects of Desiccation and Climatic Change on the Hydrology of the Aral Sea. J. Climate, **14 (3)**, 300-322.

Teschl, R. and Randeu, W. L. (2006). A neural network model for short term river flow prediction. Nat. Hazard. Earth Sys., **6 (4)**, 629-635.

Wiggin, B. L. (1950). Great snows of the Great Lakes. Weatherwise, **3 (6)**, 123-126.